© 1999 The Chemical Society of Japan Bull. Chem. Soc. Jpn., 72, 1273—1284 (1999)

Reductions of $\{RuNO\}^6$-Type Nitrosyls. Characteristics of the Two-Electron Reduction Species Isolated as a Complex Having a Formally Negatively Charged μ-Nitrosyl ($\{RuNO\}^8$–$\{RuNO\}^8$) and the One-Electron Reduction Species Generated Electrochemically ($\{RuNO\}^7$)[1)]

Hirotaka Nagao, Noriharu Nagao,[†] Yasuhiko Yukawa,[††] Dai Ooyama,[†††] Yoshinobu Sato,
Tohru Oosawa, Hiroshi Kuroda, Frank Scott Howell, and Masao Mukaida*

Department of Chemistry, Faculty of Science and Engineering, Sophia University,
Kioi-cho 7-1, Chiyoda-ku, Tokyo 102-8554

†Department of Industrial Chemistry, School of Science and Technology, Meiji University,
Higashimita 1-1-1, Kawasaki 214-0033

††Department of Enviromental Science, Faculty of Science, Niigata University, 8050 Ikarashi Nino-cho, Niigata 950-2102

†††Department of Education, Fukushima University, Matsukawa, Fukushima 960-1296

(Received December 24, 1998)

The reaction between *cis*-$[Ru(NO)(H_2O)(bpy)_2]^{3+}$ ($\{RuNO\}^6$) and formic acid gives $[\{Ru(\mu\text{-}NO)\}_2(bpy)_4]^{2+}$ (**2**) ($\{RuNO\}^8$–$\{RuNO\}^8$), along with some other products species: *cis*-$[Ru(NO)(OCHO)(bpy)_2]^{2+}$ (**1**)($\{RuNO\}^6$), and *cis*-$[Ru(OCHO)(H_2O)(bpy)_2]^+$. The μ-nitrosyl complex (**2**) consists of two *cis*-Ru(bpy)$_2$ fragments connected by two formally negatively charged bridging nitrosyl ligands. Electrochemical study of the complex shows that two successive one-electron oxidation waves to give $[\{Ru(\mu\text{-}NO)\}_2(bpy)_4]^{4+}$ ($\{RuNO\}^7$–$\{RuNO\}^7$) are found. The generated two-electron oxidation species is disintegrated to afford a one-electron reduction species, *cis*- $[Ru(NO^{\bullet})(CH_3CN)(bpy)_2]^{2+}$ ($\{RuNO\}^7$), along with a small amount of an unexpected nitro species, *cis*-$[Ru(NO_2)(CH_3CN)(bpy)_2]^+$. The characteristics of electrochemically generated one-electron reduction species *cis*-$[Ru(NO^{\bullet})X(bpy)_2]^{(n-1)+}$ ($\{RuNO\}^7$) (X = H_2O, OCHO) are investigated in the connection. During the degradation process of the one-electron reduction species, a nitrosyl-to-nitro conversion was found to proceed in *cis*-$[Ru(NO^{\bullet})(H_2O)(bpy)_2]^{2+}$, via the formation of *cis*-$[Ru(NO^{\bullet})$ $(CH_3CN)(bpy)_2]^{2+}$ mentioned above; this is the first observation which explains the electrochemically-induced nitrosyl-to-nitro conversion observed in the reduction process of $\{RuNO\}^6$-type complexes.

Metal nitrosyl complexes are of interest as models for a key material in the biological nitrite–ammonia conversion system,[2,3)] in which nitrosyl ligand-based multi-electron transfers are involved. The multi-electron transfer reaction is also important in both bio-inorganic and catalytic studies.[3—8)] Although the redox chemistry of $\{MNO\}^6$-type nitrosyl complexes has been advanced significantly, especially in connection with the study of the electrocatalytic reduction of nitrite to afford ammonia,[9—19)] much less attention has been given to the synthetic study of nitrosyl ligand reactions involving the electron transfer process, despite the necessity for better understanding of the redox behaviors of nitrosyls. Available data have shown that the species obtained synthetically via the redox process of $\{MNO\}^6$ moiety differs depending on the experimental conditions: viz. substrates, reducing agents, and other reaction conditions.[20—35)] Accordingly, the investigation of the nitrosyl ligand reaction from a synthetic standpoint still remains a research area, which should be more fully investigated.[36)] This paper describes the reaction of *cis*-$[Ru(NO)(H_2O)(bpy)_2]^{3+}$ ($\{RuNO\}^6$) with formic acid, in which the following three products were isolated. The primary product is *cis*-$[Ru(NO)(OCHO)(bpy)_2]^{2+}$ (**1**)($\{RuNO\}^6$). The second complex isolated is $[\{Ru(\mu\text{-}NO)\}_2(bpy)_4]^{2+}$ (**2**) ($\{RuNO\}^8$–$\{RuNO\}^8$), which consists of two *cis*-Ru(bpy)$_2$ fragments connected by two negative-charged bridging nitrosyl ligands. The μ-nitrosyl-ruthenium complex (**2**) is regarded as a two-electron reduction species of the original $\{RuNO\}^6$-type complex. The third product is *cis*-$[Ru(OCHO)(H_2O)(bpy)_2]^+$, which was isolated as *cis*-$[Ru(OCHO)(CH_3CN)(bpy)_2]^+$ (**3**) due to an avoidable solvation by CH_3CN. In addition to the two-electron reduction species (**2**), the characteristics of the one-electron reduction species of *cis*-$[Ru(NO)X(bpy)_2]^{n+}$ ($\{RuNO\}^6$) (X = H_2O, OCHO) were investigated; the studies of the $\{RuNO\}^7$-type complexes were done using electrochemical techniques, because their synthetic efforts were all unsuccessful, except the X = Cl complex which has been isolated under different reaction conditions.[26] A part of this work has been communicated briefly.[37]

Experimental

Materials. Raw materials (*cis*-[$RuCl_2(bpy)_2$]Cl·$2H_2O$, *cis*-[$RuCl_2(bpy)_2$]·$2H_2O$, and *cis*-[$Ru(NO_2)_2(bpy)_2$]) for these preparations were obtained by the published methods.[38,39] The following nitrosyl complexes were prepared by methods from the literature; *cis*-[$Ru(NO)X(bpy)_2$]$^{3+}$ (X = H_2O, CH_3CN),[40,41] *cis*-[$Ru(NO_2)(CH_3CN)(bpy)_2$](PF_6),[42] and *cis*-[$Ru(CH_3CN)_2(bpy)_2$]$(PF_6)_2$.[43,44] All ^{15}N labeled complexes were obtained by procedures reported in the literature.[40]

Physical Measurements. Infrared spectra were recorded with a Perkin–Elmer FT-1650 spectrophotometer. Electronic absorption spectra were recorded with a Hitachi 200 spectrophotometer. NMR spectra were recorded on a GX-270 spectrometer. Electrochemical measurements were done in CH_3CN, under an argon stream, with a supporting electrolyte (tetra-*n*-butylammonium hexafluorophosphate (TBAH) or tetraethylammonium perchlorate (TEAP), using a Huso polarograph Model 312; the current–potential waves were recorded with a Rikendenshi Instruments Model F-3F recorder. Three-electrode, one-compartment cells were used. They were equipped with a silver reference electrode (Ag | $AgNO_3$, 0.01 mol dm^{-3}). The coulometric experiments were done in two-compartment cells using a platinum-gauze working electrode, with the auxiliary electrode in the second compartment separated by a glass frit. The numbers of Coulombs were measured by a Huso Model 343B digital coulometer.

Syntheses. ***cis*-[$Ru(NO)(OCHO)(bpy)_2$]$(ClO_4)_2$ (1).** To an aqueous solution of *cis*-[$Ru(NO)(H_2O)(bpy)_2$]$(ClO_4)_3$·$3H_2O$ (200 mg/20 cm^3) in a beaker was added HCOONa (250 mg), and then the solution pH was adjusted to 4 using a few drops of formic acid. The solution was heated on a hot plate at 70 °C for 0.5 h with a cover glass, during which time the solution color changed from orange-red to pale orange. After cooling the solution, (**1**) was precipitated by adding $NaClO_4$ (100 mg). An orange crystalline material was collected by filtration, washed with water, ethanol, and then ether, and dried in vacuo. Yield 93 mg, 55%. Anal. Found: C, 36.73; H, 2.47; N, 10.02%. Calcd for $C_{21}H_{17}O_{11}N_5Cl_2Ru$: C, 36.70; H, 2.49; N, 10.19%. ^{13}C NMR (CD_3CN/TMS, ppm) δ = 167.59 (HCOO); 156.71, 155.98, 155.15, 154.71 (2,2′-bpy); 154.94, 153.92, 152.28, 149.20 (6,6′-bpy); 145.82, 145.30, 144.76, 144.23 (4,4′-bpy); 130.87, 130.46, 130.40, 130.34, 127.55, 127.14, 126.98, 126.63 (3,3′-bpy). *As a precaution with all perchlorate salts, quantities of the material were kept to a minimum for safety reasons.*

***cis*-[$Ru(NO)(OCHO)(bpy)_2$]$(PF_6)_2$·H_2O.** The corresponding PF_6 salt was prepared by the following procedure. To an aqueous solution of *cis*-[$Ru(NO)(H_2O)(bpy)_2$]$(ClO_4)_3$·$3H_2O$ (100 mg/10 cm^3) was added HCOONa (122 mg), and then the solution pH was adjusted to 4 using a few drops of formic acid. The solution was heated on a hot plate at 70 °C for 0.5 h with a cover glass, during which time the solution color changed from dark brown to bright orange. After cooling the solution, NH_4PF_6 (50 mg) was added until a reddish-orange crystalline material was deposited. The product was collected by filtration, washed with methanol and then ether, and air dried. Anal. Found: C, 31.97; H, 2.24; N, 8.42%. Calcd for $C_{21}H_{19}O_4N_5P_2F_{12}Ru$: C, 31.67; H, 2.40; N, 8.79%. Yield 53 mg, 54%.

[{Ru(*μ*-NO)}$_2$(bpy)$_4$]$(ClO_4)_2$ (2). The orange solution containing *cis*-[$Ru(NO)(OCHO)(bpy)_2$]$^{2+}$ was obtained according to the same procedure as that applied for the synthesis of (**1**). The solution species was heated further (1—2 h), without adding the precipitant, during which time the solution became black-dark brown. The solution was concentrated by gentle heating to give a black-violet crystalline material; the material includes both (**2**) and (**3**) as described below. The crude black-violet product was collected by filtration, and was purified by alumina 90 chromatography using acetonitrile as an eluent, in which two separated bands appeared. The desired product eluted as the first band (dark brown) was concentrated by rotary evaporation, and then was precipitated by adding diethyl ether (The second band was kept for the synthesis of *cis*-[$Ru(OCHO)(CH_3CN)(bpy)_2$]$^+$ (**3**)). The purified dark purple solid product was collected by filtration, then washed with diethyl ether and air dried. A typical yield for this procedure was 34%. Anal. Found: C, 43.71; H, 3.40; N, 13.02%. Calcd for $C_{40}H_{32}O_{10}N_{10}Cl_2Ru_2$: C, 44.25; H, 2.97; N, 12.90%. ^{13}C NMR (CD_3CN/TMS, ppm) δ = 157.79, 154.14 (2,2′-bpy); 150.76, 150.42 (6,6′-bpy); 139.32, 138.49 (4,4′-bpy); 127.71, 126.89 (5,5′-bpy); 124.97, 123.98 (3,3′-bpy).

[{Ru(*μ*-NO)}$_2$(bpy)$_4$]$(PF_6)_2$. To a suspension of *cis*-[$Ru(NO)(OCHO)(bpy)_2$]$(PF_6)_2$ (100 mg (0.128 mmol)) in water (10 cm^3) was added HCOONa (150 mg (2.21 mmol)), and then pH of the mixed solution was adjusted to 4, using HCOOH. The solution was refluxed in an erlenmeyer flask for 60 min, during which time the color of the solution changed from the original orange to dark purple, via the formation of a homogeneous orange solution. A crude product precipitated by addition of NH_4PF_6 (50 mg (0.306 mmol)) was collected by filtration, washed with cold water, ethanol, and then ether (dark purple crystalline material, 51 mg (Yield 27%)). The crude product was purified by alumina 90 chromatography using acetonitrile as an eluent. The desired product eluted as a first band (dark brown) was concentrated by rotary evaporation, and then was precipitated by adding diethyl ether. The purified product (purple) was collected by filtration, washed with diethyl ether, and air dried. A typical yield for this procedure was 93 mg (46%), when the experiment using 202 mg of the crude product. Anal. Found: C, 40.52; H, 2.66; N, 11.81%. Calcd for $C_{40}H_{32}O_2N_{10}P_2F_{12}Ru_2$: C, 40.82; H, 2.74; N, 11.90%.

***cis*-[$Ru(OCHO)(CH_3CN)(bpy)_2$](PF_6)·$1.5H_2O$ (3).** The second band described in the synthesis of (**2**) was collected by elution. TBAH (40 mg) was added to the elution solution and it was concentrated by evaporation, until the solution volume became 3 cm^3. Adding ether to the solution gave a reddish-brown solid material. The product was collected and washed by ether and then air dried. Yield 107 mg, 53%. Anal. Found: C, 41.18; H, 3.32; N, 10.43%. Calcd for $C_{23}H_{23}O_{3.5}N_5PF_6Ru$: C, 41.14; H, 3.45; N, 10.43%.

***cis*-[$Ru(CH_3CN)_2(bpy)_2$]$(PF_6)_2$ (4).** 100 mg (0.192 mmol) of *cis*-[$RuCl_2(bpy)_2$]·$2H_2O$ in a beaker was dissolved in the mixture of acetonitrile–water (1 : 1 v/v, 10 cm^3). The solution was heated on a hot plate using a glass cover for 1 h, and then some solid NH_4PF_6 was added. The reaction solution was left for 1 d in a refrigerator. The deposited brown material was collected by filtration, washed with water and ether, and then air dried. The product was purified by chromatography (Al_2O_3 90, CH_3CN/CH_2Cl_2 (3 : 1)). Yield 33 mg, 38%. Found: C, 36.56; H, 2.58; N, 10.75%. Calcd for $C_{24}H_{22}N_6P_2F_{12}Ru$: C, 36.70; H, 2.82; N, 10.70%.

X-Ray Structure Determination. Suitable crystals of (**1**) were obtained by slow diffusion of diethyl ether vapor into a CH_3CN solution at room temperature and dark brown crystals of (**2**) were obtained in a similar way using CH_3CN–H_2O mixed solution. Each single crystal was mounted on a glass fiber. The crystal of (**2**) was coated with manicure. The crystallographic data for both (**1**) and (**2**) are summarized in Table 1. The data for each crystal were collected by the ω–2θ scan technique ($2\theta < 55°$) on automated four-circle X-ray diffractometers (Enraf–Nonius for (**1**) and Rigaku AFC-7R for (**2**)) with graphite monochromatized Mo $K\alpha$ radiation (0.71069 Å) at 20 °C. Cell constants of both crystals were calculated by least-squares fits to the setting parameters of 25 independent reflections. All of the calculations were done on an Indy computer of Silicon graphics corporation, using TEXSAN crystallographic software package of Molecular Structure Corporation. Each structure was solved by a Patterson method and was expanded using Fourier techniques. Empirical absorption corrections using Lorentz polarization and absorption were applied. Both structures were refined with the full-matrix least-square techniques. The non-hydrogen atoms were refined anisotropically. Hydrogen atoms were placed in idealized positions and induced in structure factor calculations. The final cycle of full-matrix least-squares refinements for (**1**) was based on 5665 observations ($I < 3.00\sigma(I)$) and 361 variable parameters and those for (**2**) was based on 4887 observations ($I < 3.00\sigma(I)$) and 614 variable parameters. The atomic coordinates and thermal parameters of non-hydrogen atoms of (**1**) and (**2**) are listed in Tables 2 and 3, respectively. Tables of the atomic coordinates, thermal parameters, bond lengths and angles, and observed and calculated structure factors have been deposited as Document No. 72019 at the Office of the Editor of Bull. Chem. Soc. Jpn.

Results and Discussion

Isolation of the Reaction Products between *cis*-[Ru(NO)(H$_2$O)(bpy)$_2$]$^{3+}$ and Formic Acid. Various works on the isolation of the reduction species of {RuNO}^{6}-type nitrosyl have been developed, since Fraser and Grifith began to delve into the behavior of coordinated nitrosyl under reductive conditions.[20—30] Several reduction products, such as [{Ru(μ-NO)}$_2$Cl$_6$(SnCl$_3$)$_2$]$^{4-}$,[31] [Ru$_2$(μ-N)Cl$_8$(H$_2$O)$_2$]$^{3-}$,[31] and [{Ru(μ-NO)}$_2$(acac$_4$)] (acac = acetylacetonato),[32,35] which are related to our syntheses, have been prepared in our laboratory, in addition to both *trans*-[Ru(NO$^\bullet$)Cl(py)$_4$]$^+$ ({RuNO}^{7}) and *trans*-[Ru(NH$_3$)Cl(py)$_4$]$^+$; the latter two species correspond to the one- and six-electron reduction species respectively of *trans*-[Ru(NO)Cl(py)$_4$]$^{2+}$ ({RuNO}^{6}).[33,34] No successful isolation has been reported yet on the two-electron reduction species of the {RuNO}^{6}-type complexes. This work deals mainly with the two-electron reduction species [{Ru(μ-NO)}$_2$(bpy)$_4$]$^{2+}$ ({RuNO}^{8}–{RuNO}^{8}). Data on the complex are summarized in Table 4, along with those of some other related

Table 1. Crystallographic Data for [Ru(OCHO)(NO)(bpy)$_2$](ClO$_4$)$_2$ (**1**) and [{Ru(μ-NO)}$_2$(bpy)$_4$](ClO$_4$)$_2$ (**2**)

	1	**2**
Formula	$C_{21}H_{17}N_5O_{11}Cl_2Ru$	$C_{40}H_{32}N_{10}O_{10}Cl_2Ru_2$
FW	687.37	1085.80
Crystal system	Triclinic	Monoclinic
Space group	$P\bar{1}$	$P2_1/c$
a/Å	9.997(1)	10.791(2)
b/Å	17.112(2)	22.422(8)
c/Å	7.984(3)	20.735(2)
α/ deg	103.11(2)	
β/ deg	104.25(2)	104.363(8)
γ/ deg	80.017(10)	
V/Å^3	1279.1(5)	4859(1)
Z	2	4
Scan method	ω–2θ	ω–2θ
Scan speed/deg min^{-1}	5.7	8
T/°C	20	23
D_{calcd}/g cm^{-1}	1.79	1.48
μ(Mo $K\alpha$)/cm^{-1}	8.92	7.93
Trans. factor	0.88—1.11	0.99—1.00
$2\theta_{\max}$/deg	55.0	50.1
No. of unique data	6298	8840
No. of observed data ($I > 3.00\sigma(I)$)	5665	4887
No. of variables	361	614
R	0.034	0.056
R_{w}	0.050	0.085

Table 2. Positional Parameters and B_{eq} for [Ru(OCHO)(NO)(bpy)$_2$](ClO$_4$)$_2$ (**1**)

Atom	x	y	z	B_{eq}
Ru	0.07270(2)	−0.24280(1)	0.04323(3)	2.279(5)
Cl1	0.2924(1)	−0.00608(6)	0.1463(1)	4.54(2)
Cl2	0.3829(1)	0.35748(6)	0.6245(1)	4.57(2)
O1	0.0400(3)	−0.0998(1)	−0.1025(4)	4.03(6)
O2	−0.0400(2)	−0.3103(1)	−0.1721(3)	3.28(5)
O3	0.0152(3)	−0.2544(2)	−0.3702(3)	4.85(7)
O4	0.1847(3)	−0.0128(2)	0.2339(4)	5.23(7)
O5	0.2290(4)	0.0377(2)	0.0082(5)	7.6(1)
O6	0.4008(5)	0.0285(3)	0.2701(7)	11.6(2)
O7	0.3411(3)	−0.0865(2)	0.0658(4)	5.75(8)
O8	0.3171(9)	0.3642(4)	0.7485(9)	20.5(3)
O9	0.3069(7)	0.4158(3)	0.541(1)	18.1(2)
O10	0.5106(4)	0.3815(3)	0.6858(9)	14.6(2)
O11	0.3791(4)	0.2827(2)	0.5114(6)	8.3(1)
N1	0.0523(2)	−0.1559(1)	−0.0462(3)	2.59(5)
N2	0.1095(3)	−0.3518(1)	0.1322(3)	2.71(5)
N3	0.2452(3)	−0.3007(1)	−0.0560(3)	2.60(5)
N4	−0.0971(3)	−0.1990(2)	0.1542(4)	3.06(6)
N5	0.1677(3)	−0.1873(1)	0.2914(3)	2.77(5)
C1	−0.0418(4)	−0.3020(2)	−0.3310(5)	3.95(8)
C2	0.2008(3)	−0.4082(2)	0.0576(4)	2.84(6)
C3	0.2222(4)	−0.4867(2)	0.0870(5)	3.89(8)
C4	0.1516(5)	−0.5063(2)	0.1960(6)	4.89(10)
C5	0.0620(5)	−0.4483(2)	0.2733(6)	4.89(10)
C6	0.0417(4)	−0.3713(2)	0.2395(5)	3.88(8)
C7	0.2739(3)	−0.3805(2)	−0.0522(4)	2.91(6)
C8	0.3671(4)	−0.4295(2)	−0.1444(6)	4.42(9)
C9	0.4315(4)	−0.3978(3)	−0.2413(6)	4.88(10)
C10	0.4066(4)	−0.3164(2)	−0.2395(5)	4.35(9)
C11	0.3121(4)	−0.2697(2)	−0.1465(5)	3.41(7)
C12	−0.0698(4)	−0.1510(2)	0.3147(5)	3.39(7)
C13	−0.1782(5)	−0.1138(2)	0.3962(6)	4.94(10)
C14	−0.3137(5)	−0.1248(3)	0.3088(8)	5.9(1)
C15	−0.3387(4)	−0.1735(3)	0.1458(7)	5.4(1)
C16	−0.2299(4)	−0.2102(2)	0.0698(6)	4.24(9)
C17	0.0781(4)	−0.1434(2)	0.3916(4)	3.20(7)
C18	0.1275(5)	−0.0957(2)	0.5514(5)	4.38(9)
C19	0.2688(5)	−0.0948(2)	0.6141(5)	4.82(10)
C20	0.3589(5)	−0.1414(2)	0.5153(5)	4.44(9)
C21	0.3055(4)	−0.1866(2)	0.3525(5)	3.44(7)

Table 3. Positional Parameters and B_{eq} for $[\{\mathrm{Ru}(\mu\text{-NO})\}_2(\mathrm{bpy})_4](\mathrm{ClO_4})_2$ (**2**)

Atom	x	y	z	B_{eq}	Atom	x	y	z	B_{eq}
Ru1	0.34130(6)	0.23414(4)	0.16647(3)	3.26(2)	C7	0.330(1)	0.4213(7)	0.1891(7)	6.5(4)
Ru2	0.11122(6)	0.20632(3)	0.04898(3)	3.15(2)	C8	0.334(1)	0.4467(6)	0.1280(9)	7.2(4)
Cl1	0.9441(4)	0.0188(2)	0.2740(2)	8.2(1)	C9	0.349(1)	0.4095(6)	0.0783(7)	6.8(4)
Cl2	0.596(1)	0.1153(7)	0.4594(7)	10.7(4)	C10	0.351(1)	0.3501(5)	0.0881(6)	5.6(3)
Cl3	0.4743(7)	0.0105(4)	0.9621(5)	7.9(2)	C11	0.5843(8)	0.1686(6)	0.2028(6)	5.1(3)
O1	0.3720(6)	0.2034(4)	0.0357(3)	5.1(2)	C12	0.7128(10)	0.1507(7)	0.2133(7)	6.7(3)
O2	0.0803(6)	0.2345(4)	0.1795(4)	5.3(2)	C13	0.7989(10)	0.1958(8)	0.2023(7)	7.1(4)
O3	1.023(2)	−0.0255(9)	0.275(1)	24(1)	C14	0.756(1)	0.2490(7)	0.1816(7)	6.4(3)
O4	0.837(2)	0.0034(8)	0.2202(8)	14.3(6)	C15	0.6271(10)	0.2626(6)	0.1719(6)	5.4(3)
O5	0.998(1)	0.0741(6)	0.2625(8)	12.6(5)	C16	0.4870(10)	0.1257(6)	0.2159(6)	5.5(3)
O6	0.879(2)	0.0277(9)	0.3207(8)	16.6(7)	C17	0.512(1)	0.0692(7)	0.241(1)	9.4(5)
O7	0.625(5)	0.064(1)	0.477(2)	20(1)	C18	0.416(2)	0.0364(8)	0.255(1)	10.8(6)
O8	0.655(3)	0.136(2)	0.413(2)	16(1)	C19	0.300(1)	0.0609(7)	0.2476(8)	7.6(4)
O9	0.489(6)	0.130(3)	0.442(2)	22(2)	C20	0.2773(9)	0.1141(6)	0.2208(6)	5.3(3)
O10	0.640(4)	0.135(2)	0.521(2)	17(1)	C21	−0.0014(9)	0.0903(5)	0.0706(5)	4.1(2)
O11	0.344(3)	0.022(1)	0.952(2)	13(1)	C22	−0.008(1)	0.0306(6)	0.0859(7)	5.9(3)
O12	0.555(2)	0.0508(9)	0.944(1)	10.0(7)	C23	0.096(1)	−0.0060(6)	0.0925(8)	6.9(4)
O13	0.494(3)	0.039(1)	1.044(2)	31(1)	C24	0.209(1)	0.0192(6)	0.0835(7)	6.3(3)
N1	0.3001(7)	0.2119(3)	0.0724(4)	3.7(2)	C25	0.2125(10)	0.0786(5)	0.0691(6)	4.6(3)
N2	0.1552(7)	0.2274(3)	0.1427(4)	3.3(2)	C26	−0.1134(9)	0.1321(5)	0.0562(5)	4.1(2)
N3	0.3612(7)	0.2728(4)	0.2627(4)	4.3(2)	C27	−0.236(1)	0.1147(6)	0.0547(7)	5.8(3)
N4	0.3455(7)	0.3234(4)	0.1464(4)	4.2(2)	C28	−0.3317(10)	0.1515(7)	0.0390(7)	6.8(4)
N5	0.5434(7)	0.2227(4)	0.1824(4)	4.6(2)	C29	−0.307(1)	0.2098(7)	0.0232(7)	6.7(3)
N6	0.3675(7)	0.1493(4)	0.2046(4)	3.7(2)	C30	−0.1834(9)	0.2263(5)	0.0251(6)	5.1(3)
N7	0.1117(7)	0.1144(4)	0.0658(4)	3.7(2)	C31	0.0681(9)	0.2490(6)	−0.0891(5)	5.0(3)
N8	−0.0875(7)	0.1885(4)	0.0417(4)	4.2(2)	C32	0.051(1)	0.2506(7)	−0.1589(6)	6.4(3)
N9	0.0878(7)	0.1966(4)	−0.0552(4)	3.9(2)	C33	0.054(1)	0.1956(9)	−0.1925(6)	7.2(4)
N10	0.0723(7)	0.2937(4)	0.0157(4)	4.5(2)	C34	0.072(1)	0.1450(8)	−0.1568(7)	7.1(4)
C1	0.3566(9)	0.3319(6)	0.2628(5)	5.2(3)	C35	0.092(1)	0.1481(6)	−0.0877(5)	5.4(3)
C2	0.369(1)	0.3651(6)	0.3229(7)	6.4(4)	C36	0.056(1)	0.3024(5)	−0.0509(6)	5.3(3)
C3	0.384(1)	0.3328(9)	0.3818(6)	7.5(4)	C37	0.025(2)	0.3603(8)	−0.0760(8)	8.8(5)
C4	0.389(1)	0.2724(8)	0.3803(5)	6.1(3)	C38	0.003(2)	0.4045(8)	−0.039(1)	10.2(6)
C5	0.3767(10)	0.2440(6)	0.3220(5)	5.4(3)	C39	0.016(2)	0.3943(7)	0.027(1)	9.0(5)
C6	0.3433(9)	0.3629(5)	0.1975(6)	4.5(2)	C40	0.052(1)	0.3390(5)	0.0548(6)	5.2(3)

complexes.

The reaction of *cis*-$[\mathrm{Ru^{II}(NO^+)(H_2O)(bpy)_2}]^{3+}$ ($\{\mathrm{RuNO}\}^6$) with formic acid gave first *cis*-$[\mathrm{Ru(NO)(OCHO)(bpy)_2}]^{2+}$(**1**) ($\{\mathrm{RuNO}\}^6$). When the reaction had proceeded further, $[\{\mathrm{Ru}(\mu\text{-NO})\}_2(\mathrm{bpy})_4]^{2+}$ ($\{\mathrm{RuNO}\}^8$–$\{\mathrm{RuNO}\}^8$) (**2**) could be obtained, along with *cis*-$[\mathrm{Ru(OCHO)(H_2O)(bpy)_2}]^+$ as a precursor species of *cis*-$[\mathrm{Ru(OCHO)(CH_3CN)(bpy)_2}]^+$ (**3**). Attempting to account for the formation processes of the products ((**2**) and also (**3**)) may be useful for other related synthetic studies involving the reduction process of $\{\mathrm{RuNO}\}^6$-type complexes. Previous electrochemical study has shown that, in $\mathrm{CH_3CN}$, the starting material *cis*-$[\mathrm{Ru(NO)(H_2O)(bpy)_2}]^{3+}$ ($\{\mathrm{RuNO}\}^6$) is reduced to give *cis*-$[\mathrm{Ru(NO^\bullet)(CH_3CN)(bpy)_2}]^{2+}$ ($\{\mathrm{RuNO}\}^7$).[42] This study has shown that bond breaking occurs gradually in the (Ru–NO$^\bullet$) moiety of *cis*-$[\mathrm{Ru(NO^\bullet)(CH_3CN)(bpy)_2}]^{2+}$, when the one-electron reduction species is left at room temperature for a long time (see a later section). Under aqueous chemical conditions, however, the dimerization that gives $[\{\mathrm{Ru}(\mu\text{-NO})\}_2(\mathrm{bpy})_4]^{2+}$ ($\{\mathrm{RuNO}\}^8$–$\{\mathrm{RuNO}\}^8$) appears to occur predominantly in the one-electron reduction species, *cis*-$[\mathrm{Ru(NO^\bullet)(H_2O)(bpy)_2}]^{2+}$, via a further one-electron reduction to afford *cis*-$[\mathrm{Ru(NO^-)(H_2O)(bpy)_2}]^+$ ($\{\mathrm{RuNO}\}^8$).

When *cis*-$[\mathrm{Ru(NO)(OCHO)(bpy)_2}]^{2+}$ (**1**) ($\{\mathrm{RuNO}\}^6$), formulated as a primary product of this reaction, is changed into $[\{\mathrm{Ru}(\mu\text{-NO})\}_2(\mathrm{bpy})_4]^{2+}$ (**2**), the elimination of the OCHO ligand is necessary. Actually, the reaction to give (**2**) requires rather violent reaction conditions (in both temperature and reaction time). Yield of the reaction is also low compared with the case using *cis*-$[\mathrm{Ru(NO)(H_2O)(bpy)_2}]^{3+}$ ($\{\mathrm{RuNO}\}^6$). According to the electrochemical study described in the later section, the one-electron reduction species *cis*-$[\mathrm{Ru(NO^\bullet)(OCHO)(bpy)_2}]^+$ ($\{\mathrm{RuNO}\}^7$) undergoes a degradation, either in the (Ru–OCHO) moiety or the (Ru–NO$^\bullet$) moiety, which gives us an opportunity to obtain both *cis*-$[\mathrm{Ru(NO^\bullet)(solv)(bpy)_2}]^+$ ($\{\mathrm{RuNO}\}^7$) and *cis*-$[\mathrm{Ru(OCHO)(solv)(bpy)_2}]^+$, respectively. If we do the experiment under aqueous conditions, *cis*-$[\mathrm{Ru(NO^\bullet)(OCHO)(bpy)_2}]^+$ ($\{\mathrm{RuNO}\}^7$) will give *cis*-$[\mathrm{Ru(NO^\bullet)(H_2O)(bpy)_2}]^{2+}$ ($\{\mathrm{RuNO}\}^7$), as well as *cis*-$[\mathrm{Ru(OCHO)(H_2O)(bpy)_2}]^+$, both of which are observed in these syntheses. In this regard, we mention that $[\{\mathrm{Ru}(\mu\text{-NO})\}_2(\mathrm{bpy})_4]^{2+}$ (**2**) ($\{\mathrm{RuNO}\}^8$–$\{\mathrm{RuNO}\}^8$) once formed is relatively stable with regard to the ligand substitution, in both aqueous and nonaqueous solvents ($\mathrm{CH_3CN}$).

When the $\mathrm{CH_3CN}$ solution containing *cis*-[Ru(OCHO)-

Table 4. Complexes Isolated in the Present Reaction and the Related Complexes

Complexes	IR / cm^{-1} νNO (^{15}N labeled)	CV / V	UV-vis / nm ($\varepsilon/dm^3\,mol^{-1}cm^{-1}$)	Refs.
cis-$[Ru(NO)(OCHO)(bpy)_2](ClO_4)_2$ (**1**)	1941	$-0.23^{a)}$ $-0.99^{b)}$		
cis-$[Ru(NO)(OCHO)(bpy)_2](PF_6)_2$	1933	$-0.23^{a)}$ $-0.99^{b)}$	450 (200) 320 (18100) 292 (18900)	
$[\{Ru(\mu-NO)\}_2(bpy)_4](ClO_4)_2$ (**2**)	1363 (1332)	$-0.10^{c)}$ $0.31^{c)}$	525 (10500) 480 (11900) 292 (65700) 244 (38900)	
$[\{Ru(\mu-NO)\}_2(acac)_4]$	1575 (1543)	$-1.02^{d)}$ $-1.74^{e)}$ $0.92^{f)}$	640 (1210) 430 (2800)	35, 48
$(Me_4N)_4[\{RuNO\}_2Cl_6(SnCl_3)_2]$	1566 (1538)			31
cis-$[Ru(OCHO)(CH_3CN)(bpy)_2]PF_6$ (**3**)		$0.48^{g)}$	477 (2200) 428 (2100) 289 (19300) 241 (8060)	
cis-$[Ru(CH_3CN)_2(bpy)_2](PF_6)_2$ (**4**)		$1.10^{g)}$		

a) $E_{1/2}$ of $\{RuNO\}^6/\{RuNO\}^7$ redox couple, b) E_{pc} of $\{RuNO\}^7/\{RuNO\}^8$ reduction process, c) $E_{1/2}$ of $\{RuNO\}^8–\{RuNO\}^7/\{RuNO\}^8–\{RuNO\}^8$ and $\{RuNO\}^7–\{RuNO\}^7/\{RuNO\}^8–\{RuNO\}^7$ redox couples, d) $E_{1/2}$ of $\{RuNO\}^7–\{RuNO\}^7/\{RuNO\}^8–\{RuNO\}^7$ redox couple, e) E_{pc} of $\{RuNO\}^8–\{RuNO\}^7/\{RuNO\}^8–\{RuNO\}^8$ reduction process, f) E_{pa} of $\{RuNO\}^6–\{RuNO\}^6/\{RuNO\}^7–\{RuNO\}^7$ oxidation process, g) $E_{1/2}$ of Ru^{III}/Ru^{II} redox couple.

$(CH_3CN)(bpy)_2]^+$ (**3**) is left at room temperature, the species (**3**) changes eventually to give *cis*-$[Ru(CH_3CN)_2(bpy)_2]^{2+}$ (**4**), even at low temperatures (8—13 °C). The observed reaction progresses are summarized schematically as follows (Scheme 1).

Sequences of this reaction differ depending on the substrate used as a starting material. The experiment using the related *cis*-$[Ru(NO)(OH)(bpy)(py)_2]^{2+}$,[45] instead of *cis*-$[Ru(NO)(H_2O)(bpy)_2]^{3+}$, gave the expected *cis*-$[Ru(NO)(OCHO)(bpy)(py)_2]^{2+}$ as a primary product (this was judged by the data of both IR and CV). However, a further heating the reaction solution resulted in the elimination of the pyridine ligand to give an unidentified yellow material (precipitated as a PF_6 salt). No μ-nitrosyl complex formation was found.

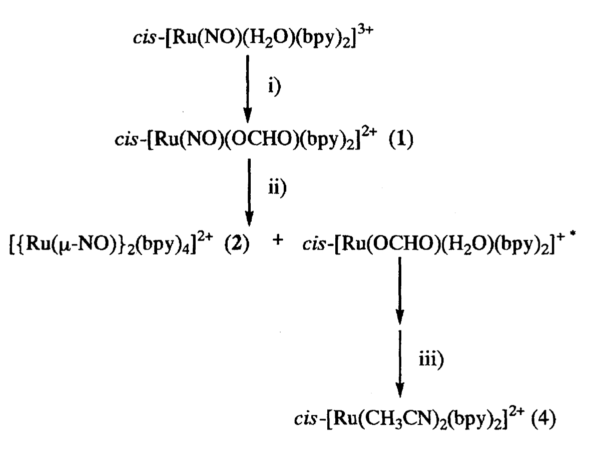

i); heated at 60 - 70 °C for 30 min. ii); heated further for totally 5 h at 60 - 70 °C. iii); kept in CH_3CN at room temperature

* We isolated the product as *cis*-$[Ru(OCHO)(CH_3CN)(bpy)_2]^+$ (3), *via* a purification process using CH_3CN.

Scheme 1. Schematic explanation for the present syntheses.

Identification, Structure, and Reactivity. Data used for the identifications are summarized in Table 4, along with those of the related complexes. All data of IR (νNO), CV, and ^{13}C NMR of *cis*-$[Ru(NO)(OCHO)(bpy)_2]^+$ (**1**), including that of the X-ray structure determination, support this formulation as a $\{RuNO\}^6$-type nitrosyl complex. Well-defined ^{13}C NMR spectra show the presence of 21 magnetically inequivalent carbon atoms; this agrees with the formula of *cis*-$[Ru(NO)(OCHO)(bpy)_2]^{2+}$, for which 20 resonances are expected from the bipyridines and 1 resonance from the formato ligand. ^1H NMR spectra showed a very similar resonance pattern to that of *cis*-$[RuXX'(bpy)_2]^n$ reported previously.[46] We did not attempt an exact assignment of each spectrum, but the total number of the protons (17) calculated by integration agreed well with the numbers expected for the formula. A proton signal due to the formato ligand appeared at $\delta = 7.89$ ppm.

ORTEP of *cis*-$[Ru(NO)(OCHO)(bpy)_2]^{2+}$ is shown in Fig. 1, along with the selected interatomic distances and angles. The cation has the expected octahedral coordination geometry. The oxygen atom of the formato ligand exists at *cis* position with respect to the nitrosyl nitrogen, and two 2,2′-bpy rings are also situated in positions *cis* to each other. The Ru–NO moiety is essentially linear with the ruthenium atom and the Ru–NO and the N–O bond lengths (1.751(3)

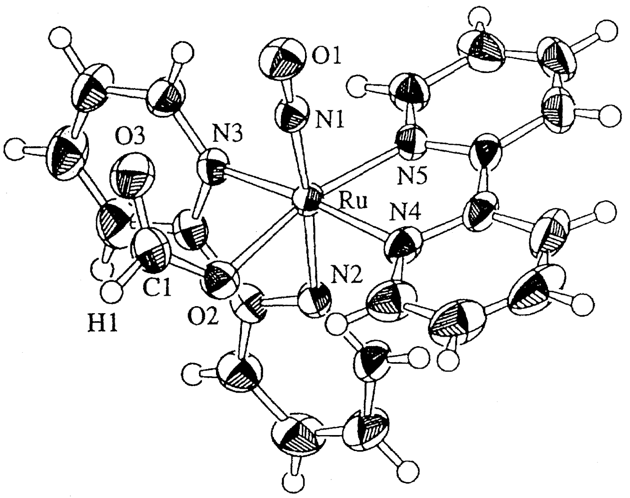

Fig. 1. ORTEP drawing of *cis*-$[Ru(NO)(OCHO)(bpy)_2]^{2+}$ with atom labeling. Carbon and hydrogen atoms of two bpy ligands are not labeled for clarity. Selected bond distances (Å) and angles (deg): Ru–N1 1.751(3), Ru–N2 2.086(3), Ru–N3 2.076(3), Ru–N4 2.056(3), Ru–N5 2.064(3), Ru–O2 2.038(2), N1–O1 1.126(3), O2–C1 1.304(4), O3–C1 1.204(5); Ru–N1–O1 179.4(2), Ru–O2–C1 121.2(2), O2–C1–O3 126.6(3).

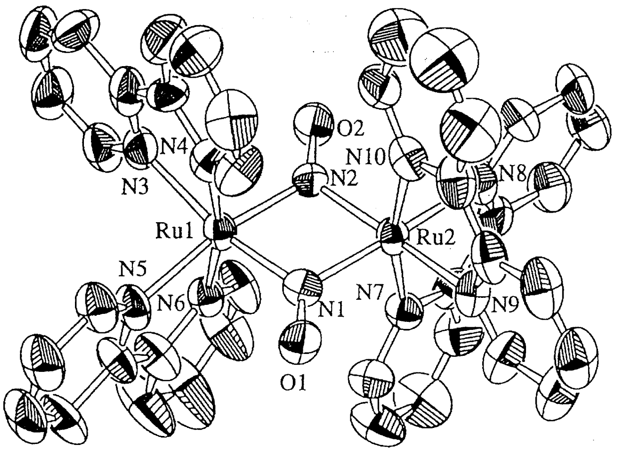

Fig. 2. ORTEP drawing of $[\{Ru(\mu\text{-}NO)\}_2(bpy)_4]^{2+}$ with atom labeling. Carbon atoms are not labeled and hydrogen atomes are omitted for clarity. Selected bond distances (Å) and angles (deg): Ru1–N1 1.954(8), Ru1–N2 1.951(7), Ru1–N3 2.137(8), Ru1–N4 2.048(9), Ru1–N5 2.139(7), Ru1–N6 2.052(8), Ru2–N1 1.979(8), Ru2–N2 1.942(7), Ru2–N7 2.089(8), Ru2–N8 2.149(8), Ru2–N9 2.123(8), Ru2–N10 2.086(9), N2–O2 1.250(9); Ru1–N1–Ru2 103.1(3), Ru1–N2–Ru2 104.6(3), Ru1–N1–O1 129.4(6), Ru1–N2–O2 127.4(6), Ru2–N1–O1 128.1(6), Ru2–N2–O2 127.4(6), N1–Ru1–N2 76.3(3), N1–Ru2–N2 76.0(3).

and 1.126(3) Å, respectively), which are similar to the values in *cis*-$[Ru(NO)Cl(bpy)_2]^{2+}$, one of the most fundamental nitrosylruthenium(II) complexes having a bipyridine ligand.[47)]

The formato moiety coordinated as a monodentate ligand is eliminated easily in solution. In a basic medium, (**1**) underwent the well-known acid-base nitro-nitrosyl conversion reaction,[6,7)] but the expected species *cis*-$[Ru(NO_2)(OCHO)(bpy)_2]$ was difficult to isolate. During purification by chromatography (Al_2O_3–CH_3CN), the species changed into a solvated species, *cis*-$[Ru(NO_2)(CH_3CN)(bpy)_2]^+$ which could be identified using an authentic sample.

The second product $[\{Ru(\mu\text{-}NO)\}_2(bpy)_4]^{2+}$ (**2**) could be characterized as a binuclear complex consisting of two *cis*-$Ru(bpy)_2$ fragments connected by two negatively-charged bridging nitrosyl ligands (NO^-) (Fig. 2), by IR, NMR, and X-Ray data. The IR absorption band due to the (νNO) is found at 1363 cm^{-1} (1340 cm^{-1} for ^{15}N labeled complex); the frequency region is considerably lower than that observed in the previous complex involving a similar $\{Ru(\mu\text{-}NO)\}_2$ fragment with a formally neutral NO ligand, $[\{Ru(\mu\text{-}NO)\}_2(acac)_4]$($\{RuNO\}^7$–$\{RuNO\}^7$) (1575 cm^{-1}), the structure of which has been established by a X-ray structure study.[48)] ^{13}C NMR results show totally 10 resonance lines; such results strongly support the characterization of the complex (**2**) as the di-μ-nitrosyl with the Λ–Λ (or Δ–Δ) form. The number of ^{13}C NMR lines observed in (**2**) indicate that the four 2,2′-ligands which coordinate to the two ruthenium atoms are all equivalent with a D_2 symmetry.

As expected by IR and NMR, the X-ray structural study shows that the complex (**2**) consists of a $\{Ru(\mu\text{-}NO)\}_2$ fragment with Λ–Λ form: Each Ru atom is approximately octahedrally coordinated by the four N atoms of two *cis*-bipyridine ligands and two nitrogen atoms of the bridging nitrosyls. The bipyridine ligands in the two halves of the dimer are arranged in a trans relationship to each other. The structure is essentially the same as $[\{Ru(\mu\text{-}NO)\}_2(acac)_4]$ except for the ancillary ligand.[48)]

The Ru–N(nitrosyl) distances average is 1.953(8) Å and is longer than that of $[\{Ru(\mu\text{-}NO)\}_2(acac)_4]$, 1.918(3) Å. The angles of Ru(1)–N(nitrosyl)–Ru(2) (103.1(3) and 104.6(3)°) are also larger than those of the acac complex, 85.7(1) and 86.1(1)°. These structural configurations are responsible for the larger Ru–Ru distance than that of the acac complex: Ru–Ru = 3.08 Å for (**2**) and 2.6143(9) Å for $[\{Ru(\mu\text{-}NO)\}_2(acac)_4]$. We judged that the Ru–Ru interaction described previously in the acac complex was negligible in the complex (**2**). The difference between the complexes is also reflected by the N–O distances of the nitrosyl groups. In the complex (**2**), the distances are 1.230(9) and 1.250(9) Å, and 1.165(3) and 1.178(3) Å in the acac complex. The result is consistent with that of the IR observation: the (νNO) of (**2**) is lower than that of $[\{Ru(\mu\text{-}NO)\}_2(acac)_4]$.

In the crystals of (**2**), there are three positions of Cl of the ClO_4^-: One of these makes an unacceptable symmetry-related pair; in the pair two of the chlorine atoms are extremely close. We did the refinement of the structure as the existence of the symmetry-related pair results from disordering, that is, the structure was refined as these two Cl atoms of the pair have a half occupancy and they connect with each other by a symmetry operation. As the result, one of two residual Cl atoms also has a half occupancy. The oxygen atoms of the ClO_4^- were treated in the reasonable way for the Cl atoms. Consequently, we decided that the total of ClO_4^- ion is two: Therefore, the formula of (**2**) is established as [{Ru-

$(\mu\text{-NO})\}_2(\mathrm{bpy})_4](\mathrm{ClO_4})_2$; the charge of the $\{\mathrm{Ru}(\mu\text{-NO})\}_2$ moiety is 2+, that is, the formal oxidation number of each Ru is 2+ and NO is 1−. The result is not contradictory to those of the other experimental data, especially electrochemical ones.

The μ-nitrosyl complex (**2**) was not stable even in a solid state. When the complex was left for a long time at room temperature, it underwent a very slow oxidation by air. When the complex (**2**) is treated by hydrochloric acidic solution, *cis*-$[\mathrm{Ru(NO)Cl(bpy)_2}]^{2+}$ ($\{\mathrm{RuNO}\}^6$) is formed almost quantitatively.

The third product *cis*-$[\mathrm{Ru(OCHO)(CH_3CN)(bpy)_2}]^+$ (**3**) was characterized tentatively. Analytical data agree well with the formula as the solvated complex, rather than with that of the aqua complex of Ru(II), *cis*-$[\mathrm{Ru(OCHO)(H_2O)(bpy)_2}]^+$. The complex shows a strong broad IR absorption band at 1577 $\mathrm{cm^{-1}}$ that is assignable to the $\nu_{\mathrm{as}}(\mathrm{COO})$ of the formato ligand. We could not detect the (νCN) in the expected region, but this is not unusual; *cis*-$[\mathrm{Ru(NO_2)(CH_3CN)(bpy)_2}]^+$ which is the authentic sample used for this study, does not show the corresponding absorption band. ^{13}C NMR spectra also indicate a *cis* configuration of the complex. As described in the above scheme, a further reaction occurs in (**3**) to give *cis*-$[\mathrm{Ru(CH_3CN)_2(bpy)_2}]^{2+}$ (**4**), by allowing *cis*-$[\mathrm{Ru(OCHO)(CH_3CN)(bpy)_2}]^+$ (**3**) to stand at room temperature. The solvated species was identified again using an authentic sample.

Redox Behaviors of the Reaction Products. The cyclic voltammogram of *cis*-$[\mathrm{Ru(NO)(OCHO)(bpy)_2}]^{2+}$ (**1**) in $\mathrm{CH_3CN}$ at 25 °C shows the behavior of a typical $\{\mathrm{RuNO}\}^6$-type nitrosyl complex: A single cathodic CV scanning had a diffusion-controlled reversible wave at −0.23 V ($E_{1/2}$), together with the coupled anodic wave on the reverse scan. Another irreversible wave appeared at the more negative potential region, −0.99 V. A controlled-potential electrolysis done at −0.30 V showed that a one-electron redox reaction proceeded ($n = 0.99$). The electrochemical behavior of (**1**) can be explained by the following Eqs. 1 and 2:

$$[\mathrm{Ru(NO)(OCHO)(bpy)_2}]^{2+} + e^- \rightleftharpoons [\mathrm{Ru(NO^{\bullet})(OCHO)(bpy)_2}]^{+} \quad (1)$$

$$[\mathrm{Ru(NO^{\bullet})(OCHO)(bpy)_2}]^{+} + e^- \rightarrow [\mathrm{Ru(NO^{-})(OCHO)(bpy)_2}] \quad (2)$$

Cyclic voltammograms of $[\{\mathrm{Ru}(\mu\text{-NO})\}_2(\mathrm{bpy})_4]^{2+}$ (**2**) measured at 25 °C in $\mathrm{CH_3CN}$ had two well-defined, reversible one-electron oxidation waves, at −0.10 and 0.31 V (vs. Ag | (0.01 mol dm^{-3} $\mathrm{AgNO_3}$) (Fig. 3). The electron transfer processes of both waves were diffusion-controlled with $i_\mathrm{p}/v^{1/2}$ constant over the range of scan rate used, and one-electron redox systems were indicated by analyses of normal pulse voltammograms. The ratios of cathodic current peak versus anodic current peak ($i_{\mathrm{pc}}/i_{\mathrm{pa}}$) for both waves were nearly unity. The observed electrochemical behavior, along with the result of a controlled-potential electrolysis described below ($n = 0.94$ for the 1st oxidation wave and $n = 1.02$ for the 2nd oxidation wave at −30 °C), can be explained if the following reactions proceed at the electrode surface (Eqs. 3 and 4):

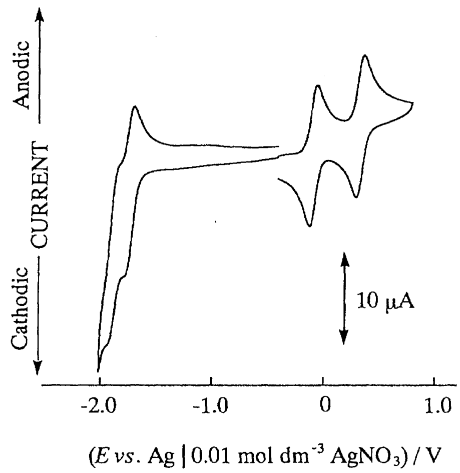

Fig. 3. Typical cyclic voltammograms (CV) of $[\{\mathrm{Ru}(\mu\text{-NO})\}_2(\mathrm{bpy})_4](\mathrm{ClO_4})_2$ (**2**).

$$[\{\mathrm{Ru}(\mu\text{-NO}^-)\}_2(\mathrm{bpy})_4]^{2+}(\{\mathrm{RuNO}\}^8\text{–}\{\mathrm{RuNO}\}^8) \rightleftharpoons$$
$$[\{\mathrm{Ru}_2(\mu\text{-NO}^{\bullet})(\mu\text{-NO}^-)\}(\mathrm{bpy})^4]^{3+}(\{\mathrm{RuNO}\}^7\text{–}\{\mathrm{RuNO}\}^8) + e^- \quad (3)$$

$$[\{\mathrm{Ru}_2(\mu\text{-NO}^{\bullet})(\mu\text{-NO}^-)\}(\mathrm{bpy})_4]^{3+}(\{\mathrm{RuNO}\}^7\text{–}\{\mathrm{RuNO}\}^8) \rightleftharpoons$$
$$[\{\mathrm{Ru}(\mu\text{-NO}^{\bullet})_2(\mathrm{bpy})_4]^{4+}(\{\mathrm{RuNO}\}^7\text{–}\{\mathrm{RuNO}\}^7) + e^- \quad (4)$$

We did the controlled-potential electrolysis at −30 °C to avoid the complexity due to the chemical reaction described later (Eq. 5), which occurred along with the oxidation reactions (Eqs. 3 and 4). When the two-electron oxidation species $[\{\mathrm{Ru}(\mu\text{-NO}^{\bullet})\}_2(\mathrm{bpy})_4]^{4+}$ ($\{\mathrm{RuNO}\}^7$–$\{\mathrm{RuNO}\}^7$) generated at −30 °C was allowed to stand at room temperature, the species underwent the degradation to give *cis*-$[\mathrm{Ru(NO^{\bullet})(CH_3CN)(bpy)_2}]^{2+}$ ($\{\mathrm{RuNO}\}^7$). Monitoring the degradation process by both CV and HDV(hydrodynamic voltammogram) indicated that $[\{\mathrm{Ru}(\mu\text{-NO}^{\bullet})\}_2(\mathrm{bpy})_4]^{4+}$ ($\{\mathrm{RuNO}\}^7$–$\{\mathrm{RuNO}\}^7$) changed within 150 min to *cis*-$[\mathrm{Ru(NO^{\bullet})(CH_3CN)(bpy)_2}]^{2+}$ ($\{\mathrm{RuNO}\}^7$) (Fig. 4). To measure the amount of product, *cis*-$[\mathrm{Ru(NO^{\bullet})(CH_3CN)(bpy)_2}]^{2+}$, we independently did a reductive exhaust electrolysis of *cis*-$[\mathrm{Ru(NO)(CH_3CN)(bpy)_2}]^{3+}$ ($\{\mathrm{RuNO}\}^6$) prepared as an authentic sample: The i_d value of the resultant *cis*-$[\mathrm{Ru(NO^{\bullet})(CH_3CN)(bpy)_2}]^{2+}$ ($\{\mathrm{RuNO}\}^7$) was compared to that of *cis*-$[\mathrm{Ru(NO^{\bullet})(CH_3CN)(bpy)_2}]^{2+}$ ($\{\mathrm{RuNO}\}^7$), which came from the exhaust oxidative electrolysis of $[\{\mathrm{Ru}(\mu\text{-NO})\}_2(\mathrm{bpy})_4]^{2+}$ (**2**). We could establish that one mole of $[\{\mathrm{Ru}(\mu\text{-NO})\}_2(\mathrm{bpy})_4]^{2+}$ (**2**) was producing two moles of *cis*-$[\mathrm{Ru(NO^{\bullet})(CH_3CN)(bpy)_2}]^{2+}$, as a result of the E–C reaction illustrated by Eqs. 3, 4, and 5.

$$[\{\mathrm{Ru}(\mu\text{-NO}^{\bullet})\}_2(\mathrm{bpy})_4]^{4+}(\{\mathrm{RuNO}\}^7\text{–}\{\mathrm{RuNO}\}^7) \rightarrow$$
$$2(cis\text{-}[\mathrm{Ru(NO^{\bullet})(CH_3CN)(bpy)_2}]^{2+}\{\mathrm{RuNO}\}^7) \quad (5)$$

Unexpectedly, small amounts of both *cis*-$[\mathrm{Ru(NO_2)(CH_3CN)(bpy)_2}]^+$ and *cis*-$[\mathrm{Ru(CH_3CN)_2(bpy)_2}]^{2+}$ were found to form during the degradation process of $[\{\mathrm{Ru}(\mu\text{-}$

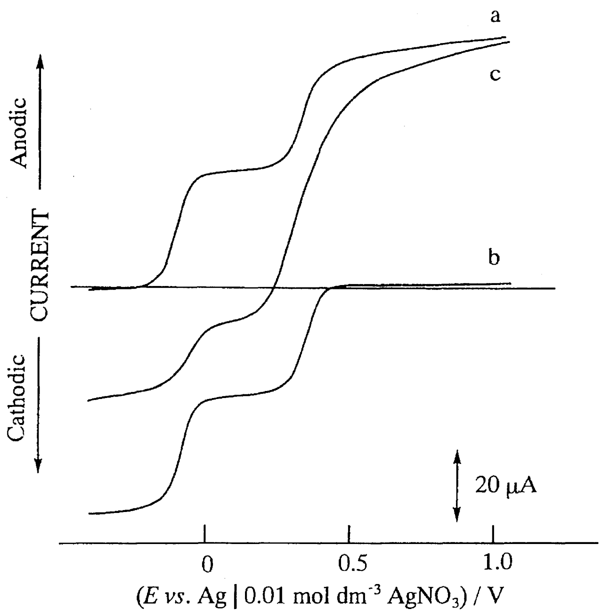

Fig. 4. Typical hydrodynamic voltammograms (HDV) of $[\{Ru(\mu\text{-}NO)\}_2(bpy)_4](ClO_4)_2$ and those of the related species. a: Before an exhaust electrolysis. b: Just after the completion of the two-electrons oxidation electrolysis which gives $[\{Ru(\mu\text{-}NO^{\bullet})\}_2(bpy)_4]^{4+}$ (The electrolysis was carried out at −30 °C). c: $[\{Ru(\mu\text{-}NO^{\bullet})\}_2(bpy)_4]^{4+}$ ($\{RuNO\}^7$–$\{RuNO\}^7$) was allowed to stand at 20 °C for 3 h, during which time *cis*-$[Ru(NO^{\bullet})(CH_3CN)(bpy)_2]^{2+}$ ($\{RuNO\}^7$) was generated ($E_{1/2}$ of *cis*-$[Ru(NO^{\bullet})(CH_3CN)(bpy)_2]^{2+/+}$ overlaps with $E_{1/2}$ of μ-nitrosyl species (**2**)).

$NO^{\bullet})\}_2(bpy)_4]^{4+}$ ($\{RuNO\}^7$–$\{RuNO\}^7$), either in the PF_6 salt of the complex having μ-nitrosyls or the ClO_4 salt.[49] Explanation for the formation of the nitro species is difficult, but the study on the characteristics of a one-electron reduction $\{RuNO\}^7$-type nitrosyl complexes described in the latter section will give some helpful information.

The CV of $[Ru(OCHO)(CH_3CN)(bpy)_2]^+$ (**3**) shows an expected reversible redox wave at 0.82 V ($E_{1/2}$), due to $[Ru(OCHO)(CH_3CN)(bpy)_2]^{2+/+}$ couple. The complex (**3**) in CH_3CN undergoes an easy substitution to give *cis*-$[Ru(CH_3CN)_2(bpy)_2]^{2+}$ (**4**); this prevented any further investigation of (**3**) in solution.

A Comparison of the Redox Behavior between $[\{Ru(\mu\text{-}NO)\}_2(bpy)_4]^{2+}$ (2) and the Related Complex $[\{Ru(\mu\text{-}NO)\}_2(acac)_4]$, Both of Which Have a Similar Binuclear Skeletal Structure. One of us has reported another di-μ-nitrosyl complex, $[\{Ru(\mu\text{-}NO)\}_2(acac)_4]$,[32,48] the molecular structure of which is essentially the same as that observed in (**2**). The $\{Ru(\mu\text{-}NO)\}_2$ fragments of both complexes, however, differ definitely in their electronic charge: (**2**) has formally NO^- ligands ($\{Ru(\mu\text{-}NO)\}_2^{2+}$ ($\{RuNO\}^8$–$\{RuNO\}^8$)), while $[\{Ru(\mu\text{-}NO)\}_2(acac)_4]$ involves formally neutral nitrosyl ligands ($\{Ru(\mu\text{-}NO)\}_2^{4+}$ ($\{RuNO\}^7$–$\{RuNO\}^7$)). Owing to the difference, the complexes show very different electrochemical behavior in their cyclic voltammograms: The previous complex $[\{Ru(\mu\text{-}NO)\}_2(acac)_4]$ ($\{RuNO\}^7$–$\{RuNO\}^7$) has shown either the oxidation wave or the reduction wave (Table 4), as represented by the following Eqs. 6, 7, and 8.[35]

For the oxidation process:

$$
\begin{aligned}
&[\{Ru(\mu\text{-}NO^{\bullet})\}_2(acac)_4](\{RuNO\}^7\text{–}\{RuNO\}^7) \\
&\quad\rightarrow [\{Ru(\mu\text{-}NO^{+})\}_2(acac)_4]^{2+}(\{RuNO\}^6\text{–}\{RuNO\}^6)+2e^- \\
&\quad\rightarrow 2[Ru(NO)(CH_3CN)(acac)_2]^{+}(\{RuNO\}^6) \qquad (6)
\end{aligned}
$$

For the reduction process:

$$
\begin{aligned}
&[\{Ru(\mu\text{-}NO^{\bullet})\}_2(acac)_4](\{RuNO\}^7\text{–}\{RuNO\}^7)+e^- \\
&\rightleftharpoons [\{Ru(\mu\text{-}NO^{\bullet})(\mu\text{-}NO^{-})\}(acac)_4]^- \times (\{RuNO\}^7\text{–}\{RuNO\}^8) \qquad (7)
\end{aligned}
$$

$$
\begin{aligned}
&[\{Ru(\mu\text{-}NO^{\bullet})(\mu\text{-}NO^{-})\}_2(acac)_4](\{RuNO\}^7\text{–}\{RuNO\}^8)+e^- \\
&\quad\rightarrow [\{Ru(\mu\text{-}NO^{-})\}_2(acac)_4]^{2-}(\{RuNO\}^8\text{–}\{RuNO\}^8) \\
&\quad\text{(decomposed)} \qquad (8)
\end{aligned}
$$

No such reduction processes were found in (**2**), as described earlier. It is reasonably assumed that the nature of the ancillary ligands (bipyridine and 2,4-pentanedione) strongly affects the stabilization of the nitrosyl ligand in each complex. A large delocalization of π-bonding over the $\{Ru(\mu\text{-}NO)\}_2$ unit will be expected in (**2**), because the bipyridine allows the $\{Ru(\mu\text{-}NO)\}_2$ unit to stabilize in a rather lower oxidation state.[50] β-Diketone anions can form very stable chelate complexes with most metal ions,[51] but the formation of such metal complexes with a lower oxidation state will not be favored.

The comproportionation constant of $[\{Ru(\mu\text{-}NO)\}_2(bpy)_4]^{2+}$ was estimated to be $\log_{10} K_{comp} = 6.93$:[52] This can be the measure for an electronic interaction through the nitrosyl bridged metal atoms.

$$
\begin{aligned}
&[\{Ru(\mu\text{-}NO^{-})\}_2(bpy)_4]^{2+}(\{RuNO\}^8\text{–}\{RuNO\}^8) \\
&\quad+[\{Ru(\mu\text{-}NO^{+})\}_2(bpy)_4]^{2+}(\{RuNO\}^6\text{–}\{RuNO\}^6) \\
&\quad\quad\rightleftharpoons [\{Ru(\mu\text{-}NO^{\bullet}\})_2(bpy)_4]^{4+}(\{RuNO\}^7\text{–}\{RuNO\}^7) \qquad (9)
\end{aligned}
$$

The related complex $[\{Ru(\mu\text{-}NO)\}_2(acac)_4]$ was not an appropriate one for the evaluation of the K_{comp} value, since the second wave was irreversible; no coupled oxidation wave was found.

Some Characteristics of the $\{RuNO\}^7$-Type Species. Redox-Induced Nitrosyl-to-Nitro Conversion Occurs in *cis*-$[Ru(NO^{\bullet})(H_2O)(bpy)_2]^{2+}$. Although various $\{MNO\}^6$-type nitrosyl complexes have been investigated,[4—7] less attention has been paid to the corresponding one-electron reduction species ($\{MNO\}^7$-type), despite its importance in molecular and electronic structures,[53] especially in the reactivity of nitrosyl compounds.[17—19] Our recent work has shown that a one-electron reduction of *cis*-$[Ru(NO)(ONO)(bpy)_n(py)_{4-2n}]^{2+}$ ($n = 1$ or 2) is followed by an easy linkage isomerization of the nitrito existing as an ancillary ligand.[39] The reverse rearrangement, from the nitro to the nitrito, is observable when the resultant nitro complex undergoes a one-electron oxidation. This electrochemical study was undertaken to investigate the chemical behaviors of $\{\mathrm{RuNO}\}^7$-type complexes, both *cis*-$[\mathrm{Ru(NO^{\bullet})(H_2O)(bpy)_2}]^{2+}$ and *cis*-$[\mathrm{Ru(NO^{\bullet})(OCHO)(bpy)_2}]^{+}$; the former was the one-electron reduction species of the starting material used for the synthesis of $[\{\mathrm{Ru}(\mu\text{-}\mathrm{NO})\}_2(\mathrm{bpy})_4]^{2+}$ (**2**) and the latter corresponded to that of *cis*-$[\mathrm{Ru(NO)(OCHO)(bpy)_2}]^{2+}$ (**1**). Such a study on the chemical behavior of the unstable $\{\mathrm{RuNO}\}^7$-type nitrosyl species has not been reported yet. Since our synthetic efforts for the one-electron reduction species were unsuccessful, except *cis*-$[\mathrm{Ru(NO^{\bullet})Cl(bpy)_2}]^{+}$ reported by Meyer et al.,[26] this experiment was done with a controlled-potential electrolysis.

Cyclic voltammograms of *cis*-$[\mathrm{Ru(NO)(H_2O)(bpy)_2}](\mathrm{PF_6})_3$ in $\mathrm{CH_3CN}$ at 25 °C had two one-electron reductions at 0.09 V (E_{pc} (1st)) and −0.71 V (E_{pc} (2nd)) (vs. Ag | $\mathrm{AgNO_3}$ (0.01 mol dm^{-3})) (Fig. 5). The one-electron redox nature of the system was indicated by an analysis of the normal pulse voltammogram. The ratio of cathodic to anodic peak current, $i_{\mathrm{pa}}/i_{\mathrm{pc}}$, for $[\mathrm{Ru(NO)(H_2O)(bpy)_2}]^{3+/2+}$ couple was nearly unity. However, the potential difference between E_{pc} and E_{pa} ($\Delta E = 140$ mV) is noticeably large as compared with the ideal Nernstian value of 59 mV for a reversible process at 25 °C; usually the related ruthenium complexes show a ΔE of 60—80 mV. The cyclic voltammogram of *cis*-$[\mathrm{Ru(NO)(H_2O)(bpy)_2}]^{3+}$ obtained by a single scanning is retained without any change, at least for few hours, unless the complex undergoes an electrolysis described below.

An easy aqua ligand substitution by $\mathrm{CH_3CN}$ occurs when the aqua species undergoes a one-electron reduction. The CV and HDV measured before and after the exhaust reductive electrolysis at 0.20 V ($n = 0.93$) show potential shift in E_{pc} (1st), while E_{pa} (1st) does not move. The cyclic voltammogram measured at the final stage of the electrolysis showed a well-shaped reversible wave at 0.19 V ($E_{1/2}$, $\Delta E = 80$ mV) (Fig. 5; solid line). The potential data thus obtained agreed well with the data of the first reduction wave of a authentic sample of *cis*-$[\mathrm{Ru(NO)(CH_3CN)(bpy)_2}](\mathrm{PF_6})_3$. The electrochemical behavior involving that of the second reduction wave can be illustrated as below:

$$[\mathrm{Ru(NO)(H_2O)(bpy)_2}]^{3+} + \mathrm{e}^- \rightleftharpoons [\mathrm{Ru(NO^{\bullet})(H_2O)(bpy)_2}]^{2+} \quad (10)$$

$$[\mathrm{Ru(NO^{\bullet})(H_2O)(bpy)_2}]^{2+} + \mathrm{CH_3CN} \rightarrow [\mathrm{Ru(NO^{\bullet})(CH_3CN)(bpy)_2}]^{2+} + \mathrm{H_2O} \quad (11)$$

$$[\mathrm{Ru(NO^{\bullet})(CH_3CN)(bpy)_2}]^{2+} + \mathrm{e}^- \rightarrow [\mathrm{Ru(NO^{-})(CH_3CN)(bpy)_2}]^{+} \quad (12)$$

To examine further how the electrochemically generated one-electron reduction species *cis*-$[\mathrm{Ru(NO^{\bullet})(H_2O)(bpy)_2}]^{2+}$ ($\{\mathrm{RuNO}\}^7$) behaves in $\mathrm{CH_3CN}$ solution when it is left at room temperature under argon stream, we attempted a monitoring experiment by a HDV. The experiment will give useful results for the illustration of the redox behavior of $[\{\mathrm{Ru}(\mu\text{-}\mathrm{NO})\}_2(\mathrm{bpy})_4]^{2+}$ (**2**), since we found that the two-electron oxidation of the complex (**2**) generates *cis*-$[\mathrm{Ru(NO^{\bullet})(CH_3CN)(bpy)_2}]^{2+}$ ($\{\mathrm{RuNO}\}^7$), before the nitrosyl-to-nitro conversion described earlier. The monitoring show first that *cis*-$[\mathrm{Ru(NO)(H_2O)(bpy)_2}](\mathrm{ClO_4})_3$ in $\mathrm{CH_3CN}$ with TEAP as a supporting electrolyte undergoes an easy solvation to give *cis*-$[\mathrm{Ru(NO^{\bullet})(CH_3CN)(bpy)_2}]^{2+}$ (Eq. 11),[49] even when the experiment was done at low temperature (−30 °C). Two more product species were formed when the temperature of the electrolyzed solution was elevated to 20—25 °C; as Fig. 6 shows, small waves appeared at 0.86 and 1.14 V, and both waves developed gradually at the expense of the wave of *cis*-$[\mathrm{Ru(NO^{\bullet})(CH_3CN)(bpy)_2}]^{2+}$. The waves

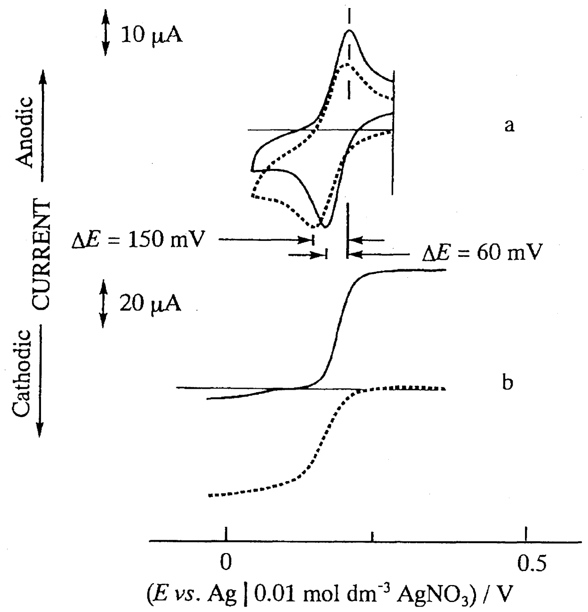

Fig. 5. CV and HDV of $[\mathrm{Ru(NO)(H_2O)(bpy)_2}]^{3+}$ in $\mathrm{CH_3CN}$. a: CV before the exhaust reductive electrolysis (dotted line) and after the exhaust reductive electrolysis ($n = 0.93$) (solid line). b: HDV before the exhaust reductive electrolysis (dotted line) and after the exhaust reductive electrolysis (solid line).

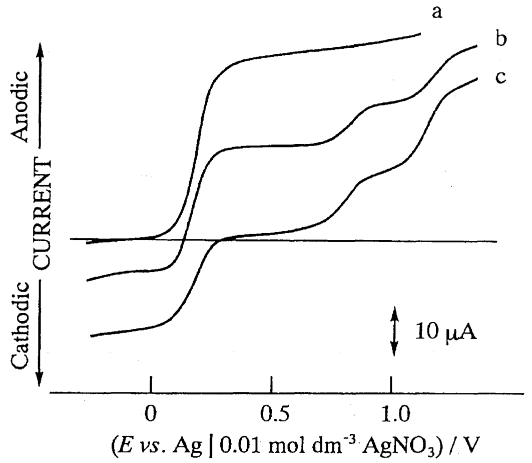

Fig. 6. Typical HDV of *cis*-$[\mathrm{Ru(NO^{\bullet})(CH_3CN)(bpy)_2}]^{2+}$ and those of the products species formed by the degradation reaction of *cis*-$[\mathrm{Ru(NO^{\bullet})(CH_3CN)(bpy)_2}]^{2+}$. a: Just after the electrolysis was completed at −30 °C. b: 6 h after standing at 20 °C, in which *cis*-$[\mathrm{Ru(NO_2)(CH_3CN)(bpy)_2}]^{+/0}$ ($E_{1/2} = 0.81$ V) and *cis*-$[\mathrm{Ru(CH_3CN)_2(bpy)_2}]^{2+/+}$ ($E_{1/2} = 1.10$ V) appeared. c: 22 h after standing at 20 °C, the waves of both species increased further.

could be ascribed to *cis*-$[\mathrm{Ru(NO_2)(CH_3CN)(bpy)_2}]^{2+}$ (for 0.86 V) and *cis*-$[\mathrm{Ru(CH_3CN)_2(bpy)_2}]^{2+}$ (for 1.14 V), using the authentic samples. Noticeably, the one-electron *oxidation* species corresponding to the original nitrosyl complex, *cis*-$[\mathrm{Ru(NO)(CH_3CN)(bpy)_2}]^{3+}$ ($\{\mathrm{RuNO}\}^6$), was generated during the progress, even though the experiment was done under an argon atmosphere in the dark.

In contrast, the related *cis*-$[\mathrm{Ru(NO^{\bullet})(OCHO)(bpy)_2}]^{+}$ shows a different monitoring pattern (Fig. 7): In addition to *cis*-$[\mathrm{Ru(NO^{\bullet})(CH_3CN)(bpy)_2}]^{2+}$ observed in the experiment of *cis*-$[\mathrm{Ru(NO^{\bullet})(H_2O)(bpy)_2}]^{2+}$, as a precursor of the nitrosyl-to-nitro conversion, the generation of *cis*-$[\mathrm{Ru(OCHO)(CH_3CN)(bpy)_2}]^{+}$ lacking a nitrosyl ligand was found. The observation indicates that bonding rupture occurs either in the Ru–NO moiety of *cis*-$[\mathrm{Ru(NO^{\bullet})(OCHO)(bpy)_2}]^{+}$ or in the Ru–OCHO moiety; the former type of bond breaking did not occur in *cis*-$[\mathrm{Ru(NO^{\bullet})(H_2O)(bpy)_2}]^{2+}$ to any appreciable amount. Similar to *cis*-$[\mathrm{Ru(NO^{\bullet})(H_2O)(bpy)_2}]^{2+}$, however, the original species *cis*-$[\mathrm{Ru(NO)(OCHO)(bpy)_2}]^{2+}$($\{\mathrm{RuNO}\}^6$) was formed as the re-oxidation product, along with a small amount of the nitro species *cis*-$[\mathrm{Ru(NO_2)(CH_3CN)(bpy)_2}]^{+}$.

It is worthy of note that, as observed in these experiments, the degradation pattern of *cis*-$[\mathrm{Ru(NO^{\bullet})X(bpy)_2}]^{n+}$ differs depending on the X ligand. Our recent study on the related *cis*-$[\mathrm{Ru(NO^{\bullet})(ONO_2)(bpy)_2}]^{+}$ ($\{\mathrm{RuNO}\}^7$) has also shown that the species gives the identical nitro species *cis*-$[\mathrm{Ru(NO_2)(CH_3CN)(bpy)_2}]^{+}$,[54] but by a definitely different reaction process, the detailed investigation of which shows that the $\mathrm{NO_3}^-$ ion acts mainly as the oxygen source of the nitrosyl-to-nitro conversion. In this context, we found that the existence of $\mathrm{ClO_4}^-$ ion did not affect the nitrosyl-to-nitro conversion; this was confirmed by an exhaust oxidative electrolysis done separately using both $\mathrm{ClO_4}^-$ and $\mathrm{PF_6}^-$ salts of (**2**) (Note that two-electron oxidation of (**2**) gives *cis*-$[\mathrm{Ru(NO_2)(CH_3CN)(bpy)_2}]^{+}$, via the formation of *cis*-$[\mathrm{Ru(NO^{\bullet})(CH_3CN)(bpy)_2}]^{2+}$ [49]).

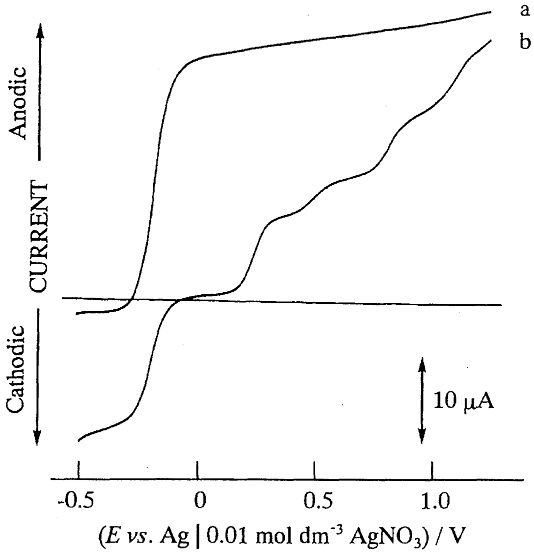

Fig. 7. Typical HDV of *cis*-$[\mathrm{Ru(NO^{\bullet})(OCHO)(bpy)_2}]^{+}$ and those of the products species formed by the degradation reaction of *cis*-$[\mathrm{Ru(NO^{\bullet})(OCHO)(bpy)_2}]^{+}$. a: Just after the electrolysis was completed at −30 °C. b: 24 h after standing at 20 °C, in which small amounts of *cis*-$[\mathrm{Ru(NO^{\bullet})(CH_3CN)(bpy)_2}]^{3+/2+}$ ($E_{1/2} = 0.19$ V), *cis*-$[\mathrm{Ru(OCHO)(CH_3CN)(bpy)_2}]^{+/0}$ ($E_{1/2} = 0.48$ V), *cis*-$[\mathrm{Ru(NO_2)(CH_3CN)(bpy)_2}]^{+/0}$ ($E_{1/2} = 0.81$ V) and *cis*-$[\mathrm{Ru(CH_3CN)_2(bpy)_2}]^{2+/+}$ ($E_{1/2} = 1.10$ V) appeared.

During the degradation processes of the $\{\mathrm{RuNO}\}^7$-type complexes, the original $\{\mathrm{RuNO}\}^6$ species was formed as the re-oxidation species in every complex of *cis*-$[\mathrm{Ru(NO^{\bullet})X(bpy)_2}]^{n+}$ ($\mathrm{X = H_2O}$ for $n = 2$, X = OCHO, $\mathrm{ONO_2}$ [54] for $n = 1$) ($\{\mathrm{RuNO}\}^7$), when their electrolyzed solutions were left at room temperature. Although *cis*-$[\mathrm{Ru(NO^{\bullet})X(bpy)_2}]^{n+}$ ($\{\mathrm{RuNO}\}^7$) are very air-sensitive species, the electrochemical experiments were done under careful conditions which protect them sufficiently from air oxidation. This was confirmed by an experiment using the related *cis*-$[\mathrm{Ru(NO^{\bullet})(NH_3)(bpy)(py)_2}]^{2+}$: The species can be retained without any marked chemical change for at least 18 h, under the same conditions.[54]

This study showed that the nitrosyl-to-nitro conversion occurred either in the *oxidative exhaust electrolysis* of $[\{\mathrm{Ru}(\mu\text{-NO})\}_2\mathrm{(bpy)_4}]^{2+}$ (**2**), or in the *reductive exhaust electrolysis* of *cis*-$[\mathrm{Ru(NO)(H_2O)(bpy)_2}]^{3+}$. *Reductive exhaust electrolysis* of *cis*-$[\mathrm{Ru(NO)(OCHO)(bpy)_2}]^{2+}$ also showed the conversion reaction, while yield of the nitro species was very low. We assume that the conversion reaction is started by the formation of *cis*-$[\mathrm{Ru(NO^{\bullet})(CH_3CN)(bpy)_2}]^{2+}$ ($\{\mathrm{RuNO}\}^7$), as the initial product of the degradation reaction (Note that the nitrosyl-to-nitro conversion does not occur in the related one-electron reduction species *cis*-$[\mathrm{Ru(NO^{\bullet})X(bpy)_2}]^{+}$ (X = OCOMe, Cl),[54] analogous to $[\mathrm{Ru(NO^{\bullet})(OCHO)(bpy)_2}]^{+}$; these species do not generate *cis*-$[\mathrm{Ru(NO^{\bullet})(CH_3CN)(bpy)_2}]^{2+}$ in any appreciable amount, while *cis*-$[\mathrm{RuX(CH_3CN)(bpy)_2}]^{+}$, lacking the nitrosyl moiety, is formed).

The redox-induced nitrosyl-to-nitro conversion observed here is extremely rare and we believe that it involves a new insight into the chemistry of nitrogen monoxide. We mention that this reaction proceeds without participating in the known types of nitrosyl-to-nitro conversion reactions; a nitrosyl-nitro acid-base equilibrium ($-\mathrm{NO^+} + 2\mathrm{OH^-} \rightarrow -\mathrm{NO_2^-} + \mathrm{H_2O}$)[6,7] and disproportionation of nitrogen monoxide ($-\mathrm{NO} + 2\mathrm{NO} \rightarrow -\mathrm{NO_2} + \mathrm{N_2O}$).[6,7] Meyer and his coworkers have mentioned first that an electrochemical reduction of *cis*-$[\mathrm{Ru(NO)(CH_3CN)(bpy)_2}]^{3+}$ might afford *cis*-$[\mathrm{Ru(NO_2)(CH_3CN)(bpy)_2}]^{+}$, along with some other unidentified product material.[55] Recently, they have also reported that the reduction of $[\mathrm{Ru(tpy)(acac)(NO)}]^{2+}$ produces the corresponding nitro species, while the product identification has not been established.[56] Noticeably, their nitrosyl-to-nitro conversions have been found in the exhaust reductive electrolyses done in the *second reduction potential* of the $\{\mathrm{RuNO}\}^6$-type complexes, although this reaction was observed in the electrolyses at the *first reduction potential* of *cis*-$[\mathrm{Ru(NO)(H_2O)(bpy)_2}]^{3+}$ ($\{\mathrm{RuNO}\}^6$] in $\mathrm{CH_3CN}$. Study is now continuing to establish the mechanistic process of the reaction. The results will be reported separately.

Conclusion

The reduction species of *cis*-$[\mathrm{Ru(NO)(H_2O)(bpy)_2}]^{3+}$ ($\{\mathrm{RuNO}\}^6$) were investigated from both synthetic and electrochemical points of views. Isolation of the one-electron reduction species was difficult under these conditions. Regardless of the difficulty, we did isolate the two-electron reduction species formulated as $[\{\mathrm{Ru}(\mu\text{-}\mathrm{NO})\}_2(\mathrm{bpy})_4]^{2+}$ (**2**); this involves the $(\{\mathrm{Ru}(\mu\text{-}\mathrm{NO})\}_2)^{2+}$ core fragment ($\{\mathrm{RuNO}\}^8$–$\{\mathrm{RuNO}\}^8$ system). The complex (**2**) has essentially the same structure as those of both $[\{\mathrm{Ru}(\mu\text{-}\mathrm{NO})\}_2(\mathrm{acac})_4]$[32,48] and $[\{\mathrm{Ru}(\mu\text{-}\mathrm{NO})\}_2\mathrm{Cl_6(SnCl_3)_2}]^{4-}$ [31] (both $\{\mathrm{RuNO}\}^7$–$\{\mathrm{RuNO}\}^7$ system) reported previously, but they differ in their formal oxidation state. A difference in the redox characteristics of the μ-nitrosyl complexes between the $\{\mathrm{RuNO}\}^7$–$\{\mathrm{RuNO}\}^7$-type and the $\{\mathrm{RuNO}\}^8$–$\{\mathrm{RuNO}\}^8$-type could be explained. In addition, a rare chemical reaction to bring about a nitrosyl-to-nitro conversion was found either in the *oxidation* of $[\{\mathrm{Ru}(\mu\text{-}\mathrm{NO})\}_2(\mathrm{bpy})_4]^{2+}$ (**2**) or in the one-electron *reduction* of *cis*-$[\mathrm{Ru(NO)(H_2O)(bpy)_2}]^{3+}$ ($\{\mathrm{RuNO}\}^6$). We could prove that the conversion in both cases proceeded via the formation of the identical species *cis*-$[\mathrm{Ru(NO^\bullet)(CH_3CN)(bpy)_2}]^{2+}$ ($\{\mathrm{RuNO}\}^7$), during the redox reaction.

We wish to thank Mr. Satoshi Igarashi (Department of Environmental Science, Niigata University) for his technical assistance in the X-ray structural analysis. This work was supported by a Grant-in-Aid for Scientific Research No. 09640622 from the Ministry of Education, Science, Sports and Culture.

References

1) The di-μ-nitrosyl complex ($[\{\mathrm{Ru(NO)(bpy)_2}\}_2]^{2+}$) which involves two formally negative charged nitrosyl moieties ($\mathrm{Ru^{II}}$–$\mathrm{NO^-}$) was abbreviated temporarily as a $\{\mathrm{RuNO}\}^8$–$\{\mathrm{RuNO}\}^8$ system for convenience. The notation is necessary, because it simplifies the illustration of the process of the degradation in (**2**), which occurs during the exhaust reductive electrolysis.

2) M. N. Hughes, "The Inorganic Chemistry of Biological Processes," 2nd ed, John Wiley & Sons, New York (1981), pp. 204—211.

3) G. B. Richter-Addo and P. Legdzine, "Metal Nitrosyls," Oxford Univ. Press., New York (1992).

4) J. H. Swinehart, *Coord. Chem. Rev.*, **2**, 385 (1967).

5) F. Bottomley, *Acc. Res.*, **11**, 158 (1978).

6) J. A. McCleverty, *Chem. Rev.*, **79**, 53 (1979).

7) F. Bottomley, *React. Coord. Ligands*, **2**, 115 (1989).

8) K. K. Pandey, *Coord. Chem. Rev.*, **51**, 69 (1983).

9) M. R. Rhodes, M. H. Barley, and T. J. Meyer, *Inorg. Chem.*, **30**, 629 (1991).

10) W. R. Murphy, Jr., K. J. Takeuchi, M. H. Barley, and T. J. Meyer, *Inorg. Chem.*, **25**, 1041 (1986).

11) M. H. Barley, K. J. Takeuchi, and T. J. Meyer, *J. Am. Chem. Soc.*, **108**, 5876 (1986).

12) W. R. Murphy, K. J. Takeuchi, and T. J. Meyer, *J. Am. Chem. Soc.*, **104**, 5817 (1982).

13) J. E. Toth and F. C. Anson, *J. Am. Chem. Soc.*, **111**, 2444 (1989).

14) S. Uchiyama and G. Muto, *J. Electroanal. Chem.*, **127**, 275 (1981).

15) K. Ogawa and H. Ishikawa, *J. Chem. Soc., Farady Trans.*, **80**, 2243 (1984).

16) I. Taniguchi, N. Nakashima, K. Matsushita, and K. Yasukouchi, *J. Electroanal. Chem.*, **224**, 199 (1987).

17) J. N. Younathan, K. S. Wood, and T. J. Meyer, *Inorg. Chem.*, **31**, 3280 (1992).

18) M. H. Barley, M. R. Rhodes, and T. J. Meyer, *Inorg. Chem.*, **26**, 1746 (1987).

19) S. W. Darryl, T. J. Meyer, and P. S. White, *J. Am. Chem. Soc.*, **117**, 823 (1995).

20) R. T. M. Fraser, *J. Chem. Soc.*, **1965**, 3641.

21) W. P. Griffith, *J. Chem. Soc.*, **1963**, 3286.

22) M. J. Clear and W. P. Griffith, *Chem. Commun.*, **1968**, 1302.

23) M. J. Clear and W. P. Griffith, *J. Chem. Soc. A*, **1970**, 1117.

24) J. N. Armor, *Inorg. Chem.*, **12**, 1959 (1973).

25) J. N. Armor and M. Z. Hoffman, *Inorg. Chem.*, **14**, 444 (1975).

26) R. W. Allahan, G. M. Brown, and T. J. Meyer, *J. Am. Chem. Soc.*, **97**, 894 (1975).

27) W. Silverthorn and R. D. Feltham, *Inorg. Chem.*, **6**, 1662 (1976).

28) R. P. Cheney and J. N. Armor, *Inorg. Chem.*, **16**, 3338 (1977).

29) P. G. Douglas and R. D. Feltham, *J. Am. Chem. Soc.*, **94**, 5254 (1971).

30) Z. Assefa and D. M. Stanbury, *J. Am. Chem. Soc.*, **119**, 521 (1997).

31) M. Mukaida, *Bull. Chem. Soc. Jpn.*, **43**, 3805 (1970). $[\mathrm{Ru_2}(\mu\text{-}\mathrm{N})\mathrm{Cl_8(H_2O)_2}]^{3-}$ has been reportd first by Griffith et al., Ref. 23.

32) M. Mukaida, T. Nomura, and T. Ishimori, *Bull. Chem. Soc. Jpn.*, **48**, 1443 (1975).

33) F. Bottomley and M. Mukaida, *J. Chem. Soc., Dalton Trans.*, **1982**, 1933.

34) K. Aoyagi, M. Mukaida, H. Kakihana, and K. Shimizu, *J. Chem. Soc., Dalton Trans.*, **1985**, 1733.

35) K. Oomura, D. Ooyama, Y. Satoh, N. Nagao, H. Nagao, F. S. Howell, and M. Mukaida, *Inorg. Chim. Acta*, **269**, 342 (1998).

36) W. P. Griffith, "The Chemistry of The Rare Platinum Metals (Os, Ru, Ir, and Rh)," John Wiley & Sons, London (1967), p. 177.

37) H. Nagao, N. Nagao, D. Ooyama, Y. Sato, T. Oosawa, H. Kuroda, F. S. Howell, and M. Mukaida, *Chem. Lett.*, **1998**, 473.

38) F. Bottomley and M. Mukaida, *Inorg. Chim. Acta*, L29 (1985).

39) J. B. Godwin and T. J. Meyer, *Inorg. Chem.*, **10**, 2150 (1971).

40) D. Ooyama, N. Nagao, H. Nagao, Y. Miura, A. Hasegawa, K. Ando, F. S. Howell, M. Mukaida, and K. Tanaka, *Inorg. Chem.*, **34**, 6024 (1995).

41) D. Ooyama, H. Nagao, K. Ito, N. Nagao, F. S. Howell, and M. Mukaida, *Bull. Chem. Soc. Jpn.*, **70**, 2141 (1997).

42) N. Nagao, D. Ooyama, K. Oomura, Y. Miura, F. S. Howell, and M. Mukaida, *Inorg. Chim. Acta*, **225**, 111 (1994).

43) G. B. Brown, R. W. Callahan, and T. J. Meyer, *Inorg. Chem.*, **14**, 1915 (1976).

44) J. L. Walsh and B. Durham, *Inorg. Chem.*, **21**, 329 (1982).

45) D. Ooyama, Y. Miura, Y. Kanazawa, F. S. Howell, N. Nagao, M. Mukaida, H. Nagao, and K. Tanaka, *Inorg. Chim. Acta*, **237**, 47

(1995).

46) D. Ooyama, N. Nagao, H. Kuroda, U. Satoh, F. S. Howell, M. Mukaida, H. Nagao, and K. Tanaka, *Bull. Chem. Soc. Jpn.*, **69**, 1593 (1996).

47) H. Nagao, D. Ooyama, F. S. Howell, M. Mukaida, and K. Mizumachi, *Anal. Sci*, **14**, 645 (1998).

48) F. Bottomley, P. S. White, and M. Mukaida, *Acta Crystallogr.*, *Sect. B*, **B38**, 2674 (1982).

49) Either in $[\{Ru(\mu\text{-}NO)\}_2(bpy)_4](ClO_4)_2$ or PF_6 salt, the yields of *cis*-$[Ru(NO_2)(CH_3CN)(bpy)_2]^+$ measured at 24 h after the electrolysis finished was estimated roughly to be 22%, by comparison with the i_d value of the authentic *cis*-$[Ru(NO_2)(CH_3CN)(bpy)_2]^+$ used as an internal standard. The yield of another product species, *cis*-$[Ru(CH_3CN)_2(bpy)_2]^{2+}$, was not obvious, since the i_d appeared near the end of the potential window, 1.4 V; this prevented the estimation of the yield of *cis*-$[Ru(CH_3CN)_2(bpy)_2]^{2+}$.

50) F. A. Cotton and G. Wilkinson, "Advanced Inorganic Chemistry, A Comprehensive Text," 4th ed, John Wiley & Sons, New York, p. 119.

51) C. M. Harris and S. E. Livingstone, "Chelating Agents and Metal Chelates," ed by E. P. Dwyer and D. P. Moellor, Academic Press, New York and London (1964), p. 95.

52) K. Kalyanasundaram and Md. K. Nazeeruddin, *Inorg. Chim. Acta*, **226**, 213 (1994).

53) H. Enemark and R. D. Feltham, *Proc. Natl. Acad. Sci. U.S.A.*, **69**, 3572 (1972).

54) In manuscript.

55) R. W. Callahan and T. J. Meyer, *Inorg. Chem.*, **16**, 574 (1977).

56) A. Dovletoglou, S. A. Adeymi, and T. J. Meyer, *Inorg. Chem.*, **35**., 4120 (1996).